Published online February 10, 2004

Nucleic Acids Research, 2004, Vol. 32, No. 3 ***1091–1096***
DOI: 10.1093/nar/gkh266

Atypical archaeal tRNA pyrrolysine transcript behaves towards EF-Tu as a typical elongator tRNA

Anne Théobald-Dietrich, Magali Frugier, Richard Giegé* and Joëlle Rudinger-Thirion

UPR 9002 du CNRS, Institut de Biologie Moléculaire et Cellulaire, 15 rue René Descartes, 67084 Strasbourg Cedex, France

Received November 25, 2003; Revised and Accepted January 15, 2004

ABSTRACT

The newly discovered tRNA^{Pyl} is involved in specific incorporation of pyrrolysine in the active site of methylamine methyltransferases in the archaeon *Methanosarcina barkeri*. In solution probing experiments, a transcript derived from tRNA^{Pyl} displays a secondary fold slightly different from the canonical cloverleaf and interestingly similar to that of bovine mitochondrial tRNA$^{Ser(UGA)}$. Aminoacylation of tRNA^{Pyl} transcript by a typical class II synthetase, LysRS from yeast, was possible when its amber anticodon CUA was mutated into a lysine UUU anticodon. Hydrolysis protection assays show that lysylated tRNA^{Pyl} can be recognized by bacterial elongation factor. This indicates that no antideterminant sequence is present in the body of the tRNA^{Pyl} transcript to prevent it from interacting with EF-Tu, in contrast with the otherwise functionally similar tRNA^{Sec} that mediates selenocysteine incorporation.

INTRODUCTION

In the methanogenic archaeal *Methanosarcina* species, methylamine methyltransferases are essential enzymes involved in methanogenesis. All known methylamine methyltransferase genes possess an in-frame amber (UAG) codon that does not stop the translation during protein synthesis (1,2); instead, a modified lysine residue, called pyrrolysine, is incorporated at these positions in the active site of the proteins (3). The mechanism by which this occurs is not yet understood, but there is a strong analogy with the selenocysteine system (4). The *Methanosarcina barkeri* genome sequence reveals the presence of the *pylT* gene, which codes for the suppressor tRNA^{Pyl}, and of three LysRS genes, one typical of class I, one of class II and the third one (*pylS*) encoding a LysRS-like protein (5). It was first proposed that, after lysylation of tRNA^{Pyl} by the *pylS* product (PylS), lysyl-tRNA^{Pyl} is converted into pyrrolysyl-tRNA^{Pyl}. However, it was recently shown that class II LysRS catalyses tRNA^{Pyl} aminoacylation in a ternary complex with class I LysRS (6), albeit the protein PylS is proposed to catalyse the modification step that produces pyrrolysyl-tRNA^{Pyl}.

To shed light on the pyrrolysine incorporation pathway, one can question whether tRNA^{Pyl} bears more resemblance to a typical elongator tRNA or to tRNA^{Sec}. The latter, after serylation by canonical SerRS and conversion into selenocysteyl-tRNA^{Sec}, binds a specialized elongation factor, the SELB protein (7), rather than EF-Tu (8) to reach the ribosomal A-site. The presence of an antideterminant box of three base pairs in the acceptor branch of bacterial tRNA^{Sec} distinguishes it from other tRNAs and is responsible for the rejection by EF-Tu (9).

The present study establishes structural features of tRNA^{Pyl} in solution and the ability of tRNA^{Pyl} transcripts to be charged by a canonical class II LysRS as well as its possible interaction with a canonical elongation factor. These functional peculiarities of tRNA^{Pyl}, which differentiate it from tRNA^{Sec}, will be discussed.

MATERIALS AND METHODS

Materials

T7 RNA polymerase (10) and EF-Tu-GDP from *Thermus thermophilus* HB8 (11) were purified from overproducing strains as described. LysRS from yeast was cloned in fusion with 6 C-terminal histidine residues in plasmid pQE70 (Qiagen), overexpressed and purified as described (12). Oligonucleotides were from Genset, radioactive L-[^{14}C]-lysine (318 mCi/mmol) was from Amersham, and phosphoenolpyruvate, pyruvate kinase and the ribonucleotides were from Boehringer. Nucleases S1, V1, T2 and T1 were from Pharmacia, USB, Invitrogen and IRL New Zealand, respectively, and lead acetate was from Merck.

Preparation of transcript and tRNA

Transcripts of tRNA^{Pyl} from *M.barkeri* were obtained by *in vitro* transcription of synthetic genes by an established procedure (13). Yeast tRNA^{Lys} transcript was prepared as described (14). Purification of the transcripts was performed by electrophoresis on preparative denaturing 12% polyacrylamide gels and elution from gel slices using a Schleicher and Schuell Biotrap apparatus (Dassel, Germany). An enriched yeast tRNA^{Lys} fraction was a gift from G. Keith (IBMC, Strasbourg).

Ultraviolet melting measurements

Melting curves of *M.barkeri* tRNA^{Pyl} and yeast tRNA^{Lys} were recorded on a Uvikon V799 spectrophotometer (Kontron Instruments). The temperature was raised from 15 to 75°C at a

*To whom correspondence should be addressed. Tel: +33 388417058; Fax: +33 388602218; Email: r.giege@ibmc.u-strasbg.fr

rate of 0.5°C/min using a Peltier system (Biotek). For measurements, tRNAs were diluted to a concentration of 0.32 µM in a buffer containing 50 mM sodium cacodylate pH 7.4, 50 mM KCl and 5 mM $MgCl_2$. Sodium cacodylate was used because it shows only slight pH variation as a function of temperature. It was verified by gel electrophoresis under denaturing conditions that the transcripts were not degraded after the melting experiments.

Structural mapping procedures

Labelling of the 5′-end of the $tRNA^{Pyl}$ transcript was performed as described previously (15). RNA was digested with various nucleases for 10 min at 20°C (for V1, S1, T1, T2) or 5 min at 50°C (for V1, T1, T2) in buffer T (100 mM KCl, 5 mM $MgCl_2$ and 50 mM HEPES–NaOH pH 7.5). For digestion with S1 nuclease, 1 mM $ZnCl_2$ was added. Reaction mixtures (10 µl) contained 50 000 c.p.m. of labelled transcript supplemented with 1 µg of unlabelled tRNA and 9×10^{-4} U RNase V1, 4.7 U RNase S1, 0.48 U RNase T1 or 0.12 U RNase T2. Reactions were stopped by immediate cooling on ice and addition of 20 µl 0.6 M NaOAc, 4 mM EDTA and 0.1 µg/µl total tRNA, followed by phenol extraction and ethanol precipitation of the tRNA.

Lead mapping was performed in buffer T at two temperatures. A freshly prepared $Pb(Oac)_2$ solution in H_2O was used at 1, 3 and 10 mM final concentrations. Samples (10 µl) were incubated for 5 min at 20°C or 1 min at 50°C. Reactions were stopped by cooling on ice, adding EDTA to a final concentration of 33 mM and ethanol precipitation.

For assignment of cleavage positions, alkaline degradations were performed by incubation of labelled transcript for 4 min at 80°C in 50 mM $NaHCO_3$ pH 9.0. Guanine ladders were generated by RNase T1 digestion under denaturing conditions (16). Controls without probes were run in parallel on each gel.

Aminoacylation assays

Before aminoacylation, transcripts were renatured by heating for 2 min at 80°C followed by slow cooling to room temperature. Lysylation of $tRNA^{Pyl}$ transcript and yeast $tRNA^{Lys}$ was performed in 100 mM HEPES–NaOH pH 7.4, 30 mM KCl, 20 mM $MgCl_2$, 2 mM ATP, 10 mM DTE, 16 µM L-[^{14}C]lysine and 5.9 µM yeast LysRS at 37°C. Kinetic parameters for $tRNA^{Pyl}$ and $tRNA^{Lys}$ were determined in the presence of 400 nM and 1 nM yeast LysRS, respectively. Transcript concentrations covered the range between 0.6 and 2.4 µM. Kinetic constants (K_m, k_{cat}) were derived from Lineweaver–Burk plots.

Hydrolysis protection assays

These experiments were conducted essentially as described before (9,17). Preparative lysylations of $tRNA^{Pyl}_{(UUU)}$ and $tRNA^{Lys}$ transcripts were performed under the conditions given above. After incubation at 37°C, reactions were stopped by phenol extraction in the presence of sodium acetate at pH 4.5. Transcripts were ethanol precipitated, washed and dried. Prior to that treatment, an aliquot of each sample was spotted on a 3MM Whatman filter and 5% trichloroacetic acid (TCA) precipitated to measure the amount of lysylated tRNAs. For the experiments, ~70 pmol of each aminoacylated transcript (taking into account the lysylation level) were dissolved in buffer H (50 mM Tris–HCl pH 7.5, 50 mM KCl, 10 mM $MgCl_2$) and incubated with 5- or 10-fold excess of EF-TuGTP in a volume of 100 µl. Controls were carried out in parallel with EF-TuGTP replaced by either EF-TuGDP or buffer H. After formation of the ternary complexes (10 min incubation on ice), samples were further incubated at 37°C to allow hydrolysis of the chemically unstable ester bond to proceed. Aliquots (20 µl) were removed after 0, 30, 60 and 90 min and spotted onto 3MM Whatman filters. After TCA precipitation, the residual radioactivity was measured by liquid scintillation counting.

RESULTS AND DISCUSSION

Structural peculiarities of $tRNA^{Pyl}$

The sequence of $tRNA^{Pyl}$ that was tentatively folded into a cloverleaf shows a number of peculiarities suggesting deviations from the canonical fold (5) (Fig. 1A). They concern the lengths of the anticodon arm and D-loop, the size of the linker between acceptor and D-arms and the number of nucleotides forming the variable region. Deviations also include the absence of the conserved G_{19} and C_{56} residues in the D- and T-loops, suggesting an atypical interaction between these two loops. Given these features, $tRNA^{Pyl}$ shares only 40% identity with conventional lysine-accepting tRNAs from *M.barkeri* (Fig. 1A) and its sequence does not contain a full lysine identity set, namely residue U_{36} present in all known lysine-accepting tRNAs. Notice, however, that the central anticodon position is occupied by a U residue, which contributes to the identity of class IIb aaRSs in *Escherichia coli* (19).

The actual fold of $tRNA^{Pyl}$ was searched *in silico* and by solution probing. The M-fold program (20) yielded various structures, including a cloverleaf. This opens the possibility that several $tRNA^{Pyl}$ transcript conformers coexist in solution, as observed for human mitochondrial $tRNA^{Lys}$. In the latter tRNA, the structural heterogeneity could be ascribed to the absence of post-transcriptional modifications that hinder formation of the correct fold (21). For $tRNA^{Pyl}$ transcripts, the coexistence of different conformers was sought by melting experiments (Fig. 2), but no evidence in support of this hypothesis was found. Indeed, the melting profile of the transcript presents rather well-defined transitions corresponding likely to the opening of the tertiary structure at 36°C and especially of a unique secondary structure at 65°C. This behaviour is also observed for yeast $tRNA^{Lys}$ transcript (Fig. 2) with, however, a 5°C download shift in the melting temperature of the cloverleaf. This difference is likely due to another distribution of G–C pairs with a strong continuous G–C stack in the acceptor stem of $tRNA^{Pyl}$.

A cloverleaf fold mimicking mitochondrial $tRNA^{Ser}$

An overall view of the single- and double-stranded regions of $tRNA^{Pyl}$ came from structure mapping using lead as the structural probe sensitive to single-stranded regions. Experiments were performed in the presence of increasing amounts of the probe at 20 and 50°C, corresponding to the presence and absence of tertiary structure based on the UV melting profile (Fig. 2). The cleavage patterns show strong cuts in the anticodon loop and variable region and weaker ones in the D- and T-loops (Fig. 3A). At 50°C, and even with a low lead concentration, all positions of the tRNA are cut, except

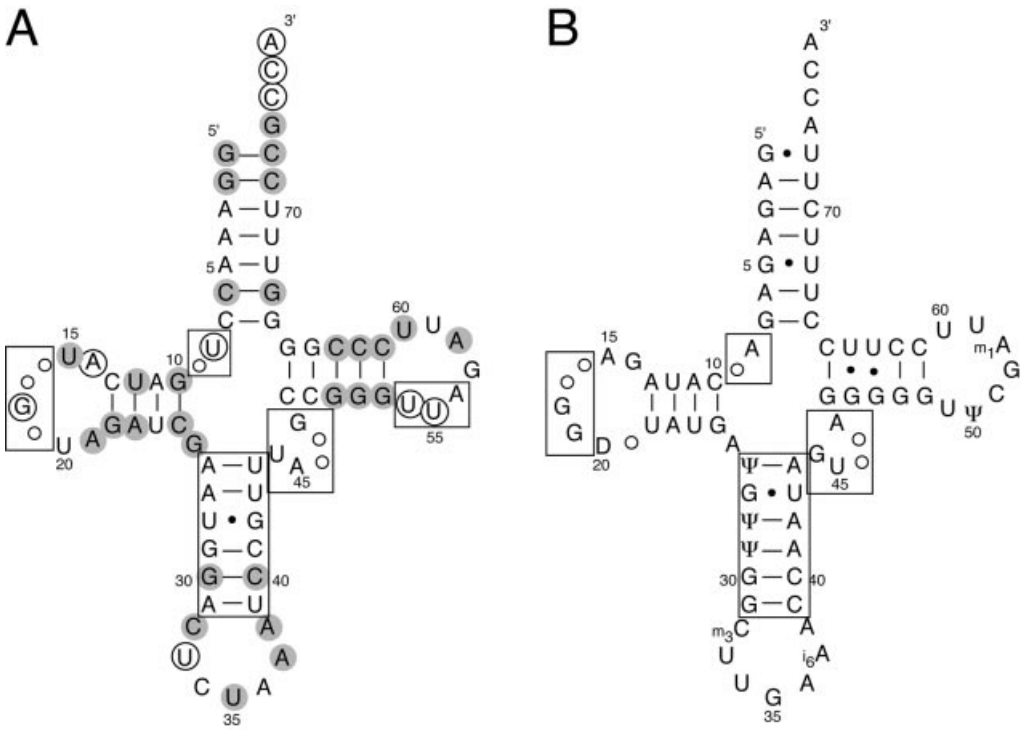

Figure 1. Cloverleaf structure of (**A**) *M.barkeri* tRNA^{Pyl} and (**B**) bovine mitochondrial tRNA^{Ser}(UGA). Numbering is according to Sprinzl *et al.* (18). Missing residues compared with canonical tRNAs are indicated by empty dots and non-canonical primary features are boxed. Consensus nucleotides in *M.barkeri* lysine-accepting tRNAs are in grey, whereas those conserved among all tRNAs are circled.

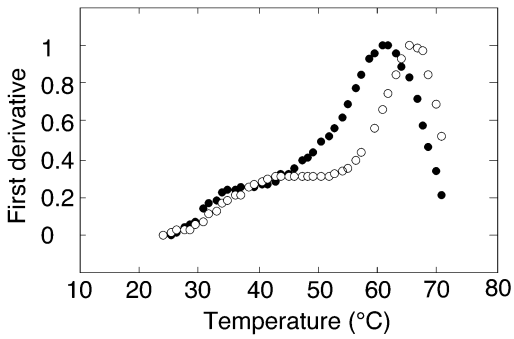

Figure 2. Melting profile of *M.barkeri* tRNA^{Pyl} and yeast tRNA^{Lys} transcripts. First derivatives of the absorption profiles obtained at 260 nm with *M.barkeri* tRNA^{Pyl} (black circles) and yeast tRNA^{Lys} (open circles) transcripts are displayed.

those in the T-arm which consists entirely of G–C pairs. In agreement with the melting experiments, these data indicate an opening of the tertiary structure as well as of the acceptor, D and anticodon stems. Additional data were obtained by probing with RNases (Fig. 3). RNase V1 cleavages agree with the existence of double-stranded acceptor, D and anticodon stems. Nuclease probing with RNase S1, T1 and T2 also supports the existence of single-stranded residues belonging to the anticodon loop, discriminator position G73 and variable region. Altogether, lead and nuclease probing confirms the cloverleaf fold depicted in Figure 1A, as previously suggested (5). A slightly different fold with an opening of the anticodon stem at base pair 27–43 was recently proposed (6), but the RNase V1 cuts in this region favour a continuous stacked anticodon branch (Fig. 3).

In contrast with canonical native elongator tRNAs (22,23), but in accordance with other *in vitro* transcripts (24), cuts by both double- and single-strand specific probes are visible in the D-loop of the tRNA^{Pyl} transcript (Fig. 3). This indicates a relaxed tertiary structure of tRNA^{Pyl}, which probably corresponds to an overall L-shaped conformation. Whether post-transcriptional modifications in tRNA^{Pyl} stabilize this conformation remains unknown.

tRNA^{Pyl} strikingly resembles bovine mitochondrial tRNA^{Ser}(UGA) (Fig. 1) which has been shown to adopt an L-shaped architecture by chemical probing and NMR (25,26). Among the five peculiarities emphasized by boxes in tRNA^{Pyl} (Fig. 1A), four exist in mitochondrial tRNA^{Ser} (Fig. 1B), namely an anticodon stem of six base pairs, a small variable region, a one-nucleotide linker between acceptor and D-arms and a reduced D-loop.

Yeast LysRS aminoacylates tRNA^{Pyl} with UUU anticodon

An unsolved question in the pyrrolysine system is whether a canonical elongation factor can recognize charged tRNA^{Pyl} or if a specialized protein is required to carry it to the ribosome. To shed light on this question, we have searched for a possible interaction between Lys-tRNA^{Pyl} and EF-Tu from *T.thermophilus*. The prerequisite to this study is the preparation of an aminoacylated tRNA^{Pyl} molecule. For that, we attempted tRNA^{Pyl} aminoacylation by yeast class II LysRS. However, because of the peculiar structure of tRNA^{Pyl} and

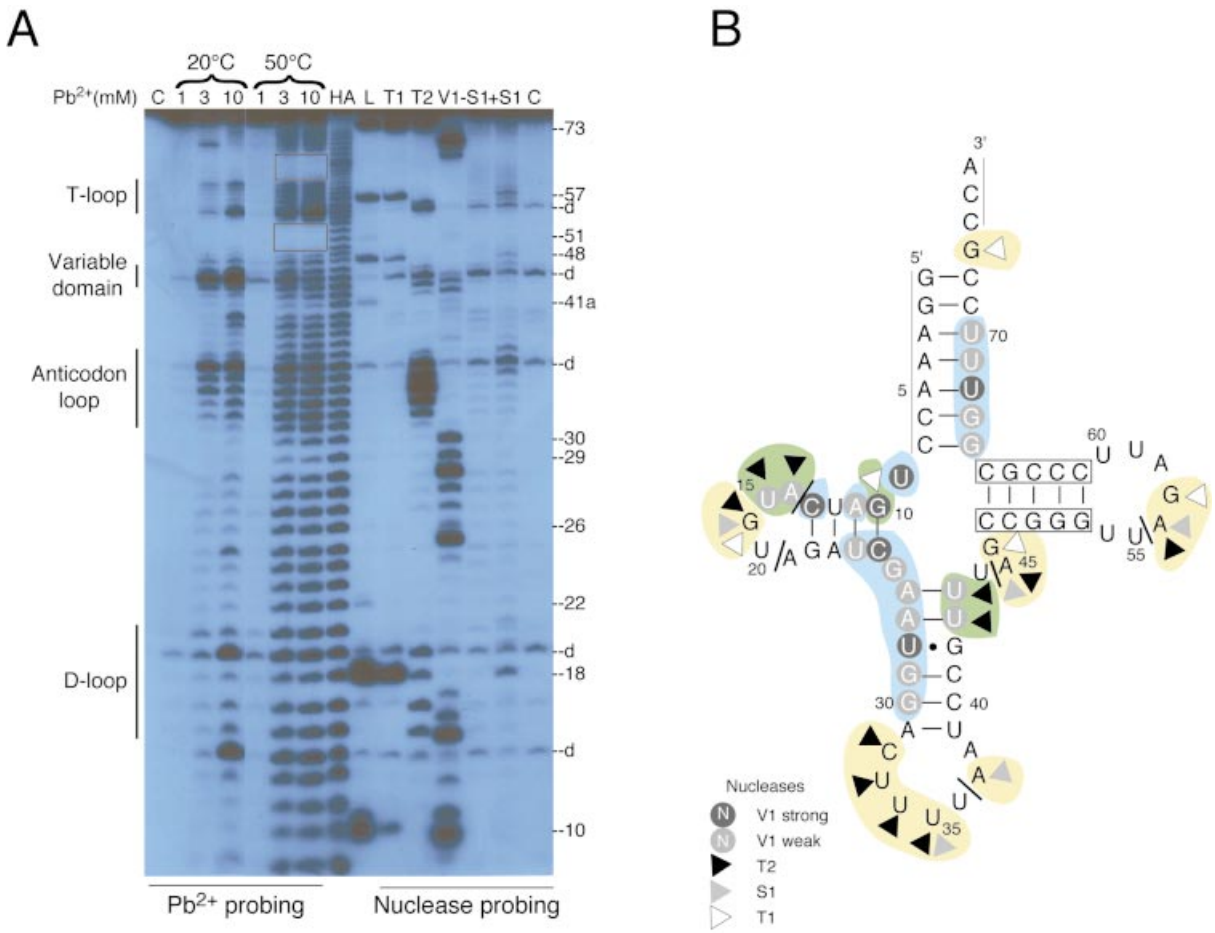

Figure 3. Probing of $tRNA^{Pyl}$ transcript. (**A**) Autoradiogram of a 12% denaturing gel of probing experiments on 5′-labelled *M.barkeri* $tRNA^{Pyl}$(UUU) transcript. Experiments using Pb^{2+} were conducted at 20 and 50°C (left part). Final concentrations of Pb^{2+} are indicated. Experiments with RNases T1, T2, V1 and S1 were conducted at 20°C (right part). Control incubations (C) were run in parallel. Lane –S1 checks the effect of $ZnCl_2$ present in nuclease S1 buffer, lane AH represents an alkaline ladder and lane L represents a denaturing RNase T1 ladder. Numbering defines the position of G residues. T-, anticodon and D-loops and the variable domain are indicated. (**B**) Summary of the probing experiments displayed on the $tRNA^{Pyl}$ cloverleaf. Lines at the 3′- and 5′-ends indicate untested regions. Nucleotides cut by nuclease S1, T1 and T2 are indicated by triangles. Cuts generated by RNase V1 are emphasized by white letters on grey or black backgrounds corresponding to weak and strong cleavages, respectively. Yellow areas correspond to nucleotides cut by probes specific of single-stranded regions and by Pb^{2+} at low temperature. Blue areas correspond to nucleotides cut by probes specific of double-stranded regions and by Pb^{2+} at high temperature. Regions cut by both types of enzymatic probes are in green. Regions resistant to Pb^{2+} cuts are boxed. Strokes indicate positions of spontaneous degradations.

Table 1. Kinetic parameters for lysylation by yeast LysRS of yeast $tRNA^{Lys}$ and *M.barkeri* $tRNA^{Pyl}$ transcripts

	K_M (nM)	k_{cat} (min^{-1})	k_{cat}/K_M (min^{-1} nM^{-1})
Yeast $tRNA^{Lys}$	12	230	19.1
M.barkeri $tRNA^{Pyl}$(CUA)	ND	ND	ND
M.barkeri $tRNA^{Pyl}$(UUU)	800	0.018	$2{,}25.10^{-5}$

ND, no lysylation detected.

also due to the presence of the CUA amber anticodon lacking U36, a major lysine identity element in *E.coli* (27), lysylation of wild-type $tRNA^{Pyl}$ seemed unlikely. This assumption was experimentally verified since no lysylation of the wild-type tRNA could be detected (Table 1). Therefore a $tRNA^{Pyl}$ mutant with a lysine UUU anticodon was produced and assayed for lysylation. As anticipated, this $tRNA^{Pyl}$ variant was a substrate for yeast LysRS, but with kinetic parameters very different from those measured with homologous $tRNA^{Lys}$ (Table 1). Despite its reduced catalytic efficiency, $tRNA^{Pyl}$(UUU) can be charged to a plateau level of 12%, dependent on the yeast LysRS concentration. Incomplete charging is not due to a high proportion of inactive molecules, but reflects an equilibrium between the aminoacylation reaction and the enzymatic or chemical deacylation reactions that catalyse hydrolysis of ester bond between lysine and $tRNA^{Pyl}$. Since the lysylation rate is low, the equilibrium leads to incomplete charging as predicted by the plateau theory (28,29).

In the context of lysylation, it is interesting that the wild-type $tRNA^{Pyl}$(CUA) is unable to inhibit $tRNA^{Pyl}$(UUU) lysylation (data not shown), indicating the importance of the UUU triplet interacting with the anticodon binding domain of yeast LysRS. This observation agrees with the recent finding that class IIb LysRS from *M.barkeri* is unable alone to lysylate

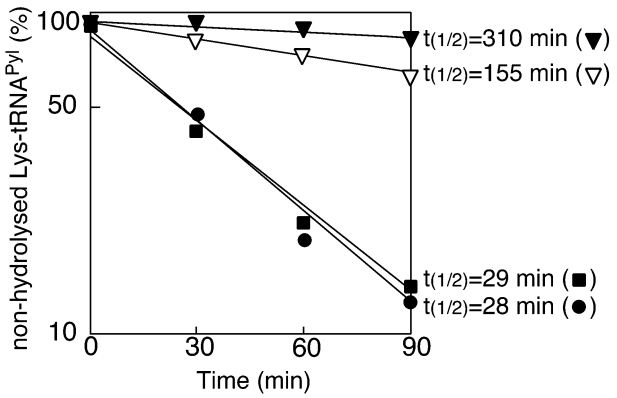

Figure 4. Interaction of EF-TuGTP with Lys-tRNA^{Pyl} transcript. Rates of hydrolysis of the lysine residue from tRNA^{Pyl}(UUU) transcript in the presence of 7 or 3.5 μM EF-TuGTP (black and open triangles, respectively), EF-TuGDP (black circles) and absence of protein (black squares). The concentrations were 0.7 μM for RNA. When used, EF-TuGDP was at 7 μM. Times required to hydrolyse 50% of the labile lysyl-ester bound ($t_{1/2}$) are indicated.

tRNA^{Pyl}(CUA) but needs a helper protein, the class I LysRS (6). This latter protein likely anchors the CUA-containing anticodon loop in the tripartite complex.

Lysylated tRNA^{Pyl} transcript interacts with EF-Tu

Biochemical data (30) and crystal structures of two ternary complexes (31,32) indicate that elongator tRNAs interact with thermophilic elongation factor Tu via their aminoacylated 3′-end, phosphorylated 5′-end and ribose phosphate backbone of their aminoacyl acceptor branch (10 first base pairs). Modified bases as well as the whole anticodon branch are not necessary for this interaction (30,33,34). These properties justify use of the tRNA^{Pyl}(UUU) transcript to model the interaction between tRNA^{Pyl} and EF-Tu.

The potential of lysylated tRNA^{Pyl} to form a ternary complex with *T.thermophilus* EF-Tu was thus tested by hydrolysis protection assays. The method is based on the fact that the activated factor protects the labile amino acid ester bond from spontaneous base-catalysed hydrolysis when bound to aminoacyl-tRNA (17). Thermophilic EF-Tu (P07157) was used in these assays because it is similar to the archaeal factor (sequence information on *M.barkeri* genome was retrieved from DDBJ/EMBL/GenBank accession number DOE_ 49338). Phylogenic comparison of EF-Tu sequences shows that conserved amino acids are essentially present in *M.barkeri* EF-Tu, including those in contact with the acceptor stem of tRNA (32). Pyrrolysine attached to tRNA would not be expected to interfere with complex formation with EF-Tu since many other unnatural amino acids of similar size can be incorporated into proteins by the canonical translational machinery (35).

Deacylation of Lys-tRNA^{Pyl} occurs in the absence of EF-Tu with a half-life of 29 min, whereas in the presence of a 10-fold (or 5-fold) excess of activated protein it is increased to 310 min (or 155 min) (Fig. 4). These variations in deacylation rates compare well with those obtained with other elongator tRNA transcripts, in particular with yeast tRNA^{Lys} transcript (data not shown). A control experiment in the presence of the inactive form of EF-Tu (EF-TuGDP) shows a deacylation rate similar to that obtained in the absence of the protein with a half-life of 28 min (Fig. 4). Taken together, these results demonstrate the ability of aminoacylated tRNA^{Pyl} to bind standard elongation factor, suggesting the absence of anti-determinant residues in the tRNA^{Pyl} framework that would hinder its recognition by EF-Tu. However, as discussed by LaRiviere *et al.* (36) and Asahara *et al.* (37), discrimination could also occur via specific thermodynamic contribution of the amino acid.

Functional implications

The above conclusions lead to unforeseen consequences if they apply to native tRNA^{Pyl}. Indeed, recognition of lysylated tRNA^{Pyl} by EF-Tu would imply its participation in protein synthesis and the incorporation of lysine at amber stop codons. The alternative would be that the lysine bound to the tRNA by the *M.barkeri* lysylation system (6) would have to be sequestered and converted into pyrrolysine in a concerted reaction after charging before interaction with EF-Tu.

In plants and fungi, exclusion of initiator tRNA^{Met} from the elongation process is due to the presence of a large 2′-phosphoribosyl modification at purine 64 in the T-stem (38,39). Since our study uses unmodified tRNA^{Pyl}, it is not excluded that a modification in native tRNA^{Pyl} at a position important for EF-Tu recognition could prevent ternary complex formation. If so, participation of a specialized elongation factor might be possible. These open questions remain to be answered by complementary experiments, in particular to determine whether modified tRNA^{Pyl} is able to interact with EF-Tu.

How far is the parallel between selenocysteine and pyrrolysine systems?

A parallel between selenocysteine and pyrrolysine incorporation into proteins was pointed out after discovery of the 22nd amino acid (4,40) because of similarities at various steps of these two translation pathways. Both use tRNAs that are first charged by standard amino acids (serine or lysine) and are then modified in a second step into non-standard derivatives (selenocysteine or pyrrolysine). The modified amino acids are then incorporated into the active site of specific proteins in response to stop codons.

The parallel is imperfect, however, since selenocysteine is incorporated in response to the UGA opal codon and pyrrolysine in response to the UAG amber codon. Further, the selenocysteine pathway is widespread in all kingdoms of life while that of pyrrolysine is restricted to certain archaea and the eubacterium *Desulfitobacterium hafniense* (5). The two systems differ also in the overall structure and size of the tRNAs, large for tRNA^{Sec} and small for tRNA^{Pyl}. Another remarkable difference is the inability of tRNA^{Sec} transcript to bind EF-Tu (8,41) while the tRNA^{Pyl} transcript, as shown in this work, can interact with this factor. Finally, we notice the puzzling resemblance of tRNA^{Pyl} with a mitochondrial tRNA^{Ser} species. Whether this mimicry is fortuitous or has evolutionary significance remains to be investigated.

ACKNOWLEDGEMENTS

We are indebted to Mathias Sprinzl (Bayreuth) for the generous gift of a clone of *T.thermophilus* EF-Tu. We thank

Eric Westhof and Benoît Masquida for useful discussion and advice, as well as Agnès Clénet for technical assistance. We are grateful to Louis Levinger for proofreading the manuscript. This work was supported by Centre National de la Recherche Scientifique and Université Louis Pasteur (Strasbourg).

REFERENCES

1. Burke,S.A., Lo,S.L. and Krzycki,J.A. (1998) Clustered genes encoding from methyltransferases of methanogenesis from monomethylamine. *J. Bacteriol.*, **180**, 3432–3440.
2. Paul,L., Ferguson,D.J. and Krzycki,J.A. (2000) The trimethylamine methyltransferase gene and multiple dimethylamine methyltransferase genes of *Methanosarcina barkeri* contain in-frame and read-through amber codons. *J. Bacteriol.*, **182**, 2520–2529.
3. Hao,B., Gong,W., Ferguson,T.K., James,C.M., Krzycki,J.A. and Chan,M.K. (2002) A new UAG-encoded residue in the structure of a methanogen methyltransferase. *Science*, **296**, 1462–1466.
4. Ibba,M. and Söll,D. (2002) Genetic code: introducing pyrrolysine. *Curr. Biol.*, **12**, R464–R466.
5. Srinivasan,G., James,C.M. and Krzycki,J.A. (2002) Pyrrolysine encoded by UAG in archaea: charging of a UAG-decoding specialized tRNA. *Science*, **296**, 1459–1462.
6. Polycarpo,C., Ambrogelly,A., Ruan,B., Tumbula-Hansen,D., Ataide,S.F., Ishitani,R., Yokoyama,S., Nureki,O., Ibba,M. and Söll,D. (2003) Activation of the pyrrolysine suppressor tRNA requires formation of a ternary complex with class I and class II lysyl-tRNA synthetases. *Mol. Cell*, **12**, 287–294.
7. Commans,S. and Böck,A. (1999) Selenocysteine inserting tRNAs: an overview. *FEMS Microbiol. Rev.*, **23**, 335–351.
8. Förster,C., Ott,G., Forchhammer,K. and Sprinzl,M. (1990) Interaction of a selenocysteine-incorporating tRNA with elongation factor Tu from *E.coli*. *Nucleic Acids Res.*, **18**, 487–491.
9. Rudinger,J., Hillenbrandt,R., Sprinzl,M. and Giegé,R. (1996) Antideterminants present in minihelix^{Sec} hinder its recognition by prokaryotic elongation factor Tu. *EMBO J.*, **15**, 650–657.
10. Becker,H.D., Giegé,R. and Kern,D. (1996) Identity of prokaryotic and eukaryotic tRNA^{Asp} for aminoacylation by aspartyl-tRNA synthetase from *Thermus thermophilus*. *Biochemistry*, **35**, 7447–7458.
11. Limmer,S., Reiser,C.O.A., Schirmer,N.K., Grillenbeck,N.W. and Sprinzl,M. (1992) Nucleotide binding and GTP hydrolysis by elongation factor Tu from *Thermus thermophilus* as monitored by proton NMR. *Biochemistry*, **31**, 2970–2977.
12. Frugier,M., Moulinier,L. and Giegé,R. (2000) A domain in the N-terminal extension of class IIb eukaryotic aminoacyl-tRNA synthetases is important for tRNA binding. *EMBO J.*, **19**, 2371–2380.
13. Perret,V., Garcia,A., Grosjean,H., Ebel,J.-P., Florentz,C. and Giegé,R. (1990) Relaxation of transfer RNA specificity by removal of modified nucleotides. *Nature*, **344**, 787–789.
14. Korencic,D., Söll,D. and Ambrogelly,A. (2002) A one-step method for *in vitro* production of tRNA transcripts. *Nucleic Acids Res.*, **30**, e105.
15. Silberklang,M., Gillum,A.M. and RajBhandary,U.L. (1977) The use of nuclease P1 in sequence analysis of end group labeled RNA. *Nucleic Acids Res.*, **4**, 4091–4108.
16. Peattie,D.A. and Gilbert,W. (1980) Chemical probes for higher-order structure in RNA. *Proc. Natl Acad. Sci. USA*, **77**, 4679–4682.
17. Pingoud,A. and Urbanke,C. (1980) Aminoacyl transfer ribonucleic acid binding site of the bacterial elongation factor Tu. *Biochemistry*, **19**, 2108–2112.
18. Sprinzl,M., Horn,C., Brown,M., Ioudovitch,A. and Steinberg,S. (1998) Compilation of tRNA sequences and sequences of tRNA genes. *Nucleic Acids Res.*, **26**, 148–153.
19. Giegé,R., Sissler,M. and Florentz,C. (1998) Universal rules and idiosyncratic features in tRNA identity. *Nucleic Acids Res.*, **26**, 5017–5035.
20. Zucker,M. (1989) On finding suboptimal foldings of an RNA molecule. *Science*, **244**, 48–52.
21. Helm,M., Giegé,R. and Florentz,C. (1999) A Watson–Crick base-pair disrupting methyl group (m^1A9) is sufficient for cloverleaf folding of human mitochondrial tRNA^{Lys}. *Biochemistry*, **38**, 13338–13346.
22. Boutorin,A.S., Clark,B.F.C., Ebel,J.-P., Kruse,T.A., Petersen,H.U., Remy,P. and Vassilenko,S. (1981) A study of the interaction of *Escherichia coli* elongation factor Tu with aminoacyl-tRNAs by partial digestion with cobra venom ribonuclease. *J. Mol. Biol.*, **152**, 593–608.
23. Théobald,A., Springer,M., Grunberg-Manago,M., Ebel,J.-P. and Giegé,R. (1988) Tertiary structure of *Escherichia coli* tRNA^{Thr3} in solution and interaction of this tRNA with the cognate threonyl-tRNA synthetase. *Eur. J. Biochem.*, **175**, 511–524.
24. Sissler,M., Eriani,G., Martin,F., Giegé,R. and Florentz,C. (1997) Mirror image alternative interaction patterns of the same tRNA with either class I arginyl-tRNA synthetase or class II aspartyl-tRNA synthetase. *Nucleic Acids Res.*, **25**, 4899–4906.
25. Watanabe,Y.-I., Kawai,G., Yokogawa,T., Hayashi,N., Kumazawa,Y., Ueda,T., Nishikawa,K., Hirao,I., Miura,K.-I. and Watanabe,K. (1994) Higher-order structure of bovine mitochondrial tRNA^{Ser}(UGA): chemical modification and computer modeling. *Nucleic Acids Res.*, **22**, 5378–5384.
26. Hayashi,I., Kawai,G. and Watanabe,K. (1998) Higher-order structure and thermal instability of bovine mitochondrial tRNA^{Ser}(UGA) investigated by proton NMR spectroscopy. *J. Mol. Biol.*, **284**, 57–69.
27. Tamura,K., Himeno,H., Asahara,H., Hasegawa,T. and Shimizu,M. (1992) *In vitro* study of *E.coli* tRNA^{Arg} and tRNA^{Lys} identity. *Nucleic Acids Res.*, **20**, 2335–2339.
28. Bonnet,J. and Ebel,J.-P. (1972) Interpretation of incomplete reactions in tRNA aminoacylation. Aminoacylation of yeast tRNA^{Val}II with yeast valyl-tRNA synthetase. *Eur. J. Biochem.*, **31**, 335–344.
29. Dietrich,A., Kern,D., Bonnet,J., Giegé,R. and Ebel,J.-P. (1976) Interpretation of tRNA-mischarging kinetics. *Eur. J. Biochem.*, **70**, 147–158.
30. Rudinger,J., Blechschmidt,B., Ribeiro,S. and Sprinzl,M. (1994) Minimalist aminoacylated RNAs as efficient substrates for elongation factor Tu. *Biochemistry*, **33**, 5682–5688.
31. Nissen,P., Kjeldgaard,M., Thirup,S., Polekhina,G., Reshetnikova,L., Clark,B.F.C. and Nyborg,J. (1995) Crystal structure of the ternary complex of Phe-tRNA^{Phe}, EF-Tu and a GTP analog. *Science*, **270**, 1464–1472.
32. Nissen,P., Thirup,S., Kjeldgaard,M. and Nyborg,J. (1999) The crystal structure of Cys-tRNA^{Cys}-EF-TuGDPNP reveals general and specific features in the ternary complex and in tRNA. *Structure*, **7**, 143–156.
33. Nazarenko,I.A., Harrington,K.M. and Uhlenbeck,O.C. (1994) Many of the conserved nucleotides of tRNA^{Phe} are not essential for ternary complex formation and peptide elongation. *EMBO J.*, **13**, 2464–2471.
34. Nazarenko,I.A. and Uhlenbeck,O.C. (1995) Defining a smaller RNA substrate for elongation factor Tu. *Biochemistry*, **34**, 2545–2552.
35. Liu,D.R. and Schultz,P.G. (1999) Progress towards the evolution of an organism with an expanded genetic code. *Proc. Natl Acad. Sci. USA*, **96**, 4780–4785.
36. LaRiviere,F.J., Wolfson,A.D. and Uhlenbeck,O.C. (2001) Uniform binding of aminoacyl-tRNAs to elongation factor Tu by thermodynamic compensation. *Science*, **294**, 165–168.
37. Asahara,H. and Uhlenbeck,O.C. (2002) The tRNA specificity of *Thermus thermophilus* EF-Tu. *Proc. Natl Acad. Sci. USA*, **99**, 3499–3504.
38. Kiesewetter,S., Ott,G. and Sprinzl,M. (1990) The role of modified purine 64 in initiator/elongator discrimination of tRNA^{Meti} from yeast and wheat germ. *Nucleic Acids Res.*, **18**, 4677–4682.
39. Aström,S. and Byström,A.S. (1994) Rit1, a tRNA backbone-modifying enzyme that mediates initiator and elongator tRNA discrimination. *Cell*, **79**, 535–546.
40. Atkins,J.F. and Gesteland,R.F. (2002) The 22nd amino acid. *Science*, **296**, 1409–1410.
41. Baron,C. and Böck,A. (1991) The length of the aminoacyl-acceptor stem of the selenocysteine-specific tRNA^{Sec} of *Escherichia coli* is the determinant for binding to elongation factors SELB or Tu. *J. Biol. Chem.*, **266**, 20375–20379.